frontiers in Chemistry

ORIGINAL RESEARCH
published: 20 September 2021
doi: 10.3389/fchem.2021.733350

Crassifolins Q–W: Clerodane Diterpenoids From *Croton crassifolius* With Anti-Inflammatory and Anti-Angiogenesis Activities

Canjie Li[1†], Xin Sun[1,2†], Wenjing Yin[3], Zhaochun Zhan[1], Qing Tang[1], Wenzhi Wang[1], Xuefang Zhuo[1], Zhongnan Wu[2], Haipeng Zhang[3], Yaolan Li[1], Yubo Zhang[1,3]* and Guocai Wang[1]**

[1]Guangdong Province Key Laboratory of Pharmacodynamic Constituents of TCM and New Drugs Research, Institute of Traditional Chinese Medicine and Natural Products, College of Pharmacy, Jinan University, Guangzhou, China, [2]The First Affiliated Hospital of Jinan University, Guangzhou, China, [3]Department of Pharmacology, School of Medicine, Guangdong Clinical Translational Center for Targeted Drug, Jinan University, Guangzhou, China

Seven new clerodane diterpenoids, crassifolins Q–W (**1**–**7**), along with five known analogues (**8**–**12**), were isolated from the roots of *Croton crassifolius*. Their structures were identified by comprehensive spectroscopic analysis (UV, IR, NMR, and HR-ESI-MS), and their absolute configurations were determined by ECD spectra and X-ray crystallography. The activities of compounds **1**–**5** against inflammatory cytokines IL-6 and TNF-α levels on LPS-induced RAW 264.7 macrophages were assessed, and compound **5** showed the most significant activity with the secretion levels of IL-6 and TNF-α at 32.78 and 12.53%, respectively. Moreover, compounds **1**–**5** were screened for their anti-angiogenesis using a human umbilical vein endothelial cells *in vitro* mode; the results showed all of them exhibited obvious anti-angiogenesis activities, in particular, compound **5** showed the strongest anti-angiogenesis effect in the range of 6.25–50 μM.

Keywords: Euphorbiaceae, *Croton crassifolius*, clerodane diterpenoids, anti-inflammatory activity, anti-angiogenic activity

OPEN ACCESS

Edited by:
Simone Brogi,
University of Pisa, Italy

Reviewed by:
Fateh V Singh,
VIT University, India
Assem Barakat,
King Saud University, Saudi Arabia
Ben W Greatrex,
University of New England, Australia
Haruhisa Kikuchi,
Tohoku University, Japan

***Correspondence:**
Yaolan Li
tliyl@jnu.edu.cn
Yubo Zhang
ybzhang99@126.com
Guocai Wang
twangguocai@jnu.edu.cn

†These authors have contributed equally to this work and share first authorship

Specialty section:
This article was submitted to Medicinal and Pharmaceutical Chemistry, a section of the journal Frontiers in Chemistry

Received: *30 June 2021*
Accepted: *02 August 2021*
Published: *20 September 2021*

Citation:
Li C, Sun X, Yin W, Zhan Z, Tang Q, Wang W, Zhuo X, Wu Z, Zhang H, Li Y, Zhang Y and Wang G (2021) Crassifolins Q–W: Clerodane Diterpenoids From Croton crassifolius *With Anti-Inflammatory and Anti-Angiogenesis Activities. Front. Chem. 9:733350. doi: 10.3389/fchem.2021.733350*

INTRODUCTION

The genus *Croton* (Euphorbiaceae) is a rich source of diterpenoids with interesting structural diversity such as clerodane-type (Campos et al., 2010; Khanitha and Damrong, 2011; Sun et al., 2014), kauritan-type (Dao et al., 2011; Suwancharoen et al., 2012), heliurane-type (Martha et al., 2011; Huang et al., 2014a), phorbol ester-type (Zhang et al., 2013; Corlay et al., 2014), and trachylobane-type (Martinsen et al., 2010). These diterpenoids exhibited remarkable biological characteristics including anti-inflammatory (Wang et al., 2015), anti-tumor (Fernandes et al., 2013; Young et al., 2013; Maslovskaya et al., 2015), anti-viral (Nina et al., 2014), anti-bacterial (Liu et al., 2014), and anti-oxidation activities (Mariana et al., 2013), which make them particularly valuable for phytochemical and pharmacological research studies. *Croton crassifolius* Geisel (Euphorbiaceae) is well known as "Jiguxiang" and mainly distributed in the south and southwest area of China, such as Guangxi, Guangdong, and Hainan provinces. The roots of the *C. crassifolius* are used as a traditional medicine for treatment of joint pain, rheumatic arthritis, stomach ache, pharyngitis, and jaundice (Boonyarathanakornkit et al., 1988). Previous phytochemical studies on *C. crassifolius* showed that the derivatives of diterpenoids were the main active ingredients (Huang et al., 2014b; Li et al., 2014).

TABLE 1 | ^{1}H NMR data of **1–7** (δ in ppm, J in Hz)[a].

Position	1	2	3	4	5	6	7
1	1.84, m	α 2.34, m	1.65, m	1.95, m	2.06, m	—	α 3.09, d (17.1)
	—	β 1.96, m	—	—	—	—	β 2.66, m
2	α 2.14, m	1.70, m	1.61, m	α 1.71, m	1.34, m	2.56, m	—
	β 1.85, m	—	—	β 1.51, m	—	—	—
3	α 2.07, m	α 2.09, m	α 2.03, m	1.94, m	α 1.83, m	α 2.43, m	α 2.70, m
	β 1.45, m	β 1.80, m	β 1.42, m	—	β 1.35,m	β 2.17, m	β 2.26, d (17.1)
4	—	—	—	—	—	3.97, t (4.6)	—
6	α 1.67, m	5.46, t (8.2)	α 2.07, m	1.96, m	4.99, t (8.1)	—	α 1.75, m
	β 1.47, m	—	β 1.97, m	—	—	—	β 1.68, d (9.6)
7	α 1.92, m	α 2.10, m	α 1.73, m	α 1.50, m	α 2.09, m	α 2.90, dd (16.3, 10.7)	α 1.68, d (9.6)
	β 1.70, m	β 1.87, m	β 1.46, m	β 1.35, m	β 1.63, m	β 2.44, m	β 1.42, m
8	2.70, dd (10.2, 4.3)	1.89, m	1.78, m	1.72, m	1.97, m	2.22, m	1.97, m
11	α 2.04, m	α 2.87, dd (14.5, 8.7)	1.74, m	1.62, m	1.69, m	α 2.71, dd (12.3, 9.0)	2.79, s
	β 1.92, m	β 2.34, m	—	—	—	β 2.18, m	—
12	α 2.54, t (13.9)	5.46, t (8.2)	α 2.41, m	α 2.22, m	2.31, m	5.90, t (7.5)	—
	β 2.01, m		β 1.98, m	β 2.01, m	—	—	—
14	6.29, s	6.50, s	5.82, s	—	5.82, s	6.40, s	6.75, s
15	7.35, s	7.54, s	—	4.75, d (1.8)	—	7.44, s	8.05, s
16	7.22, s	7.62, s	4.75, s	7.10, s	4.72, s	7.46, s	7.41, s
17	—	1.05, d (6.4)	α 4.38, dd (11.0, 4.3)	0.88, d (6.8)	α 0.98, d (7.2)		0.99, d (6.5)
	—	—	β 3.83, t (9.2)	—	β 1.32, s	—	—
18	—	—	—	—	—	—	—
19	1.30, s	9.89, s	1.27, s	1.29, s		1.14, d (7.0)	1.08, s
20	1.12, s		1.00, s	0.87, s	1.02, s	—	1.20, s
22	—	1.92, s	—	—	—	—	—
23	—	—	6.83, d (7.0)	—	—	—	—
24	—	—	1.77, d (7.0)	—	—	—	—
25	—	—	1.78, s	—	—	—	—
18-OCH_3	—	3.68, s	—	—	—	3.68, s	—

[a]*All measured in CDCl3 at 400 MHz.*

In our early research studies, the investigations on *C. crassifolius* had led to the isolation of some new diterpenoids (Wang et al., 2012; Wang et al., 2016). However, the diterpenoids from their work showed relatively moderate biological activities including anti-HSV and anti-angiogenesis. In order to search more bioactive natural products from *Croton* plants, the phytochemical investigation on the roots of *C. crassifolius* was performed, leading to the isolation of seven new clerodane diterpenoids, named crassifolins Q–W (**1**–**7**), along with five known compounds, EBC-205 (**8**) (Maslovskaya et al., 2019), mallotucin B (**9**) (Takashi et al., 1976), crassin D (**10**) (Yuan et al., 2017), spiro [furan-3(2*H*),6'-(6*H*)naphtho (1,8-bc)furan]-2'a (2'*H*)-carboxylic acids (**11**) (Nakatsu et al., 1981; Li et al., 2019), and crassifolin H (**12**) (Qiu et al., 2016).

Considering the potential anti-inflammatory activity of clerodane diterpenoids (Zhang et al., 2019), we evaluated the inhibitory effects of diterpenoids **1**–**5** on inflammation by testing the secretion level of inflammatory cytokines IL-6 and TNF-α on LPS-stimulated RAW 264.7 cells. In earlier research papers, inflammation has anti-cancer effects, which can affect the host immune response, help the body recognize and kill cancer cells, and can be used in anti-cancer immunotherapy (Bryant, 1868). However, in recent years, more and more studies have shown that inflammation can promote the occurrence and development of cancer under most conditions and reduce the therapeutic effect of tumors (Francescone et al., 2014; Moses et al., 2018). Furthermore, the formation of new vessels and angiogenesis are important processes of tumor growth and metastasis. On this basis, we want to isolate compounds that can exhibit anti-inflammatory and anti-angiogenesis activities simultaneously, so as to act as lead compounds to interfere with inflammation and cancer. Moreover, a previous study (Wang et al., 2016) reported that some diterpenoids of this plant exhibited potential activity on anti-angiogenesis, which inspired us to conduct an anti-angiogenesis activity on compounds **1**–**5** using a human umbilical vein endothelial cell (HUVEC) *in vitro* mode. Herein, this article reported the isolation, structural elucidation, and evaluation of anti-inflammatory and anti-angiogenic activities of the new compounds.

RESULTS AND DISCUSSION

Characterization of Compounds

Compound **1** was isolated as a colorless crystal. Its molecular formula was deduced as $C_{20}H_{26}O_5$ on the basis of its HR-ESI-MS data [*m/z* 369.1660 $(M + Na)^+$, calcd for $C_{20}H_{26}O_5Na$, 369.1672]. The IR spectrum suggested the presence of hydroxyl (3,463 cm^{-1}), carbonyl (1710 cm^{-1}), and furan ring (1,461, 867 cm^{-1}) in the structure of **1**. The ^{1}H NMR spectrum (**Table 1**) revealed the presence of three olefinic protons [δ_H 7.35 (1H, s), 7.22 (1H, s), and 6.29 (1H, s)] and two methyl groups [δ_H 1.30 (3H, s) and 1.12 (3H, s)]. The ^{13}C NMR and DEPT spectra (**Table 2**) showed 20 carbons including two carboxyl

TABLE 2 | ^{13}C NMR data of **1–7** (δ in ppm)[a].

Position	1	2	3	4	5	6	7
1	21.7, CH2	26.1, CH2	24.8, CH2	25.2, CH2	22.8, CH2	199.9, C	43.7, CH2
2	24.9, CH2	17.6, CH2	20.0, CH2	19.6, CH2	18.5, CH2	35.4, CH2	205.7, C
3	36.6, CH2	28.7, CH2	36.6, CH2	35.6, CH2	29.2, CH2	24.4, CH2	45.9, CH2
4	47.7, C	59.2, C	47.6, C	47.5, C	41.7, C	38.7, CH	51.0, C
5	131.8, C	129.8, C	133.2, C	131.4, C	131.6, C	144.9, C	76.6, C
6	20.1, CH2	71.7, CH	27.5, CH2	25.9, CH2	74.7, CH	198.6, C	32.8, CH2
7	37.4, CH2	32.7, CH2	22.2, CH2	26.8, CH2	31.3, CH2	41.7, CH2	24.9, CH2
8	46.5, CH	36.2, CH	39.0, CH	33.4, CH	32.7, CH	37.9, CH	35.8, CH
9	40.9, C	54.1, C	40.5, C	40.9, C	39.4, C	48.8, C	44.0, C
10	135.3, C	138.2, C	134.6, C	135.8, C	136.2, C	145.9, C	89.0, C
11	27.1, CH2	40.5, CH2	33.9, CH2	34.4, CH2	36.9, CH2	41.6, CH2	44.4, CH2
12	19.7, CH2	72.6, CH	23.7, CH2	20.5, CH2	24.2, CH2	72.7, CH	194.4, C
13	125.3, C	125.0, C	171.0, C	135.2, C	170.1, C	125.4, C	129.7, C
14	111.2, CH	108.1, CH	115.3, CH	174.5, CH	115.6, CH	108.3, CH	108.9, CH
15	142.9, CH	144.4, CH	174.2, C	70.2, CH2	173.9, C	144.3, CH	147.7, CH
16	138.7, CH	139.6, CH	73.3, CH2	143.9, CH	73.1, CH2	139.2, CH	144.5, CH
17	181.1, C	16.6, CH3	65.7, CH2	16.1, CH3	15.6, CH3	175.2, C	17.5, CH_3
18	183.7, C	172.2, C	182.7, C	182.7, C	180.7, C	171.3, C	176.6, C
19	24.4, CH3	196.7, CH	24.4, CH3	23.1, CH3	21.0, CH3	16.0, CH3	14.0, CH_3
20	23.0, CH3	176.7, C	21.4, CH3	21.0, CH3	22.2, CH3	—	15.3, CH_3
21	—	170.1, C	168.4, C	—	—	—	—
22	—	21.1, CH3	128.8, C	—	—	—	—
23	—	—	137.6, CH	—	—	—	—
24	—	—	14.5, CH3	—	—	—	—
25	—	—	12.2, CH3	—	—	—	—
18-OCH_3	—	52.6, CH3	—	—	—	52.9, CH3	—

[a]*All measured in CDCl3 at 100 MHz.*

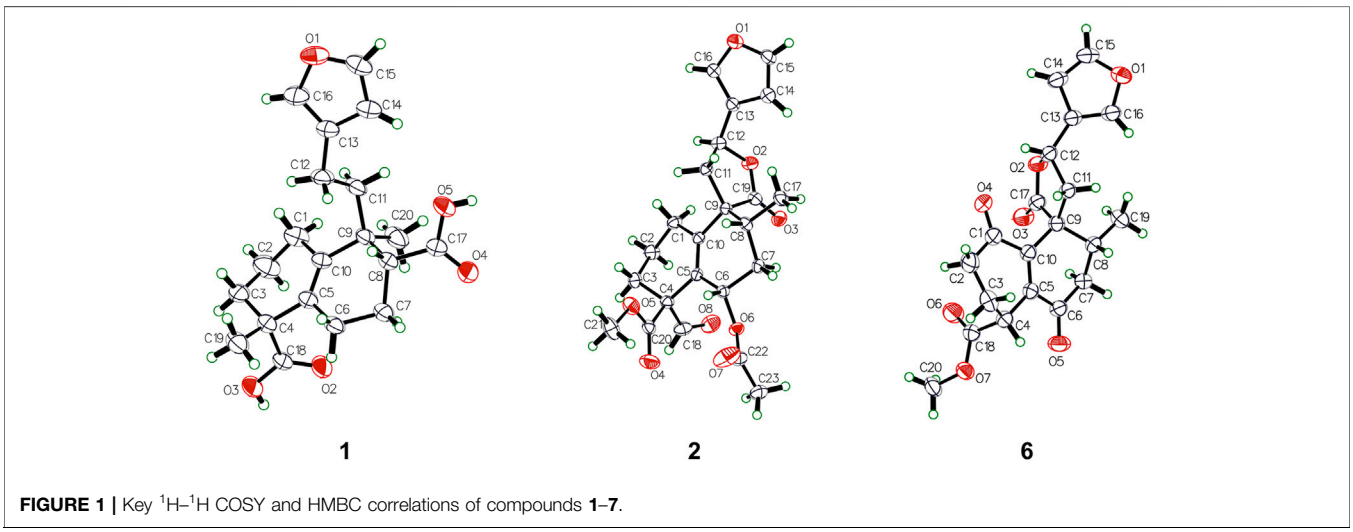

FIGURE 1 | Key ^1H–^1H COSY and HMBC correlations of compounds **1–7**.

carbons (δ_C 183.7 and 181.1), five quaternary carbons, seven methylenes, four methines, and two methyls, suggesting that **1** is a clerodane diterpenoid with a comparable structure to the known compound crassifolin B (Wang et al., 2012). The major differences between **1** and crassifolin B were the absence of a methyl (δ_C 16.3, C-17) and a γ-lactone ring, but the presence of a carboxylic acid group (δ_C 181.1) and a β-substituted furan ring, and the chemical shifts of C-13 to C-17 shifted from δ_C 171.2, 115.2, 174.2, 73.3, 16.3 to δ_C 125.3, 111.2, 142.9, 138.7, 181.1, respectively. These differences suggested that the γ-lactone in crassifolin B was replaced by a β-substituted furan ring in **1**, which was verified by the ^1H–^1H COSY correlation between H-14 (δ_H 6.29) and H-15 (δ_H 7.35) and the HMBC cross peaks from H-12 (δ_H 2.04) to C-13 (δ_C 125.3)/C-14 (δ_C 111.2)/C-16 (δ_C 138.7) and from H-16 (δ_H 7.22) to C-13/C-14/C-15 (**Figure 1**). In addition, the ^1H–^1H COSY correlations of H-6 (δ_H 1.47)/H-7 (δ_H 1.92) and H-7/H-8 (δ_H 2.70), along with the HMBC cross peaks from H-8 to C-9 (δ_C 40.9)/C-17 (δ_C 181.1)/C-20 (δ_C 23.0) were observed, which could confirm that the carboxylic acid group was attached to C-8 (**Figure 1**). Furthermore, to establish

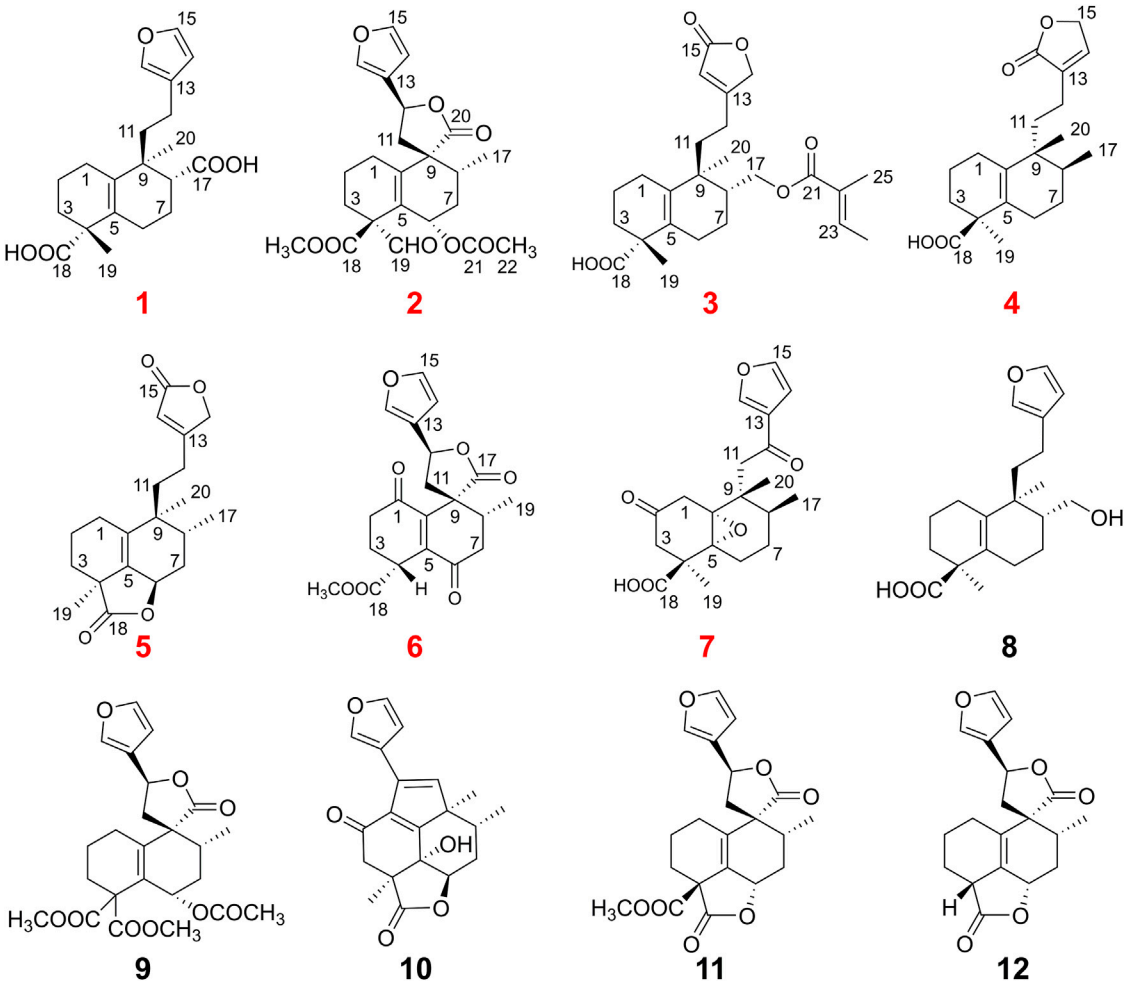

FIGURE 2 | The X-ray ORTEP drawing of compounds **1**, **2**, and **6**.

the stereochemistry of **1**, the single crystals were obtained in a chloroform system and subjected to an X-ray diffraction experiment with Cu Kα radiation. The crystal data [Flack parameter -0.1 (3), hooft parameter -0.3 (3)] determined the absolute configuration of **1** as 4*R*, 8*R*, 9*S* (**Figure 2**). Consequently, the structure was determined and named as crassifolin Q.

Compound **2** was obtained as a colorless crystal and the HR-ESI-MS showed an $[M + Na]^+$ ion peak at *m/z* 453.1506 (calcd for $C_{23}H_{26}O_8Na$, 453.1520), consistent with the molecular formula of $C_{23}H_{26}O_8$. The ^1H NMR spectrum (**Table 1**) showed apparent signals for an aldehyde proton [δ_H 9.89 (1H, s)], three olefinic protons [δ_H 7.62 (1H, s), 7.54 (1H, s), and 6.50 (1H, s)], two oxygenated methines [δ_H 5.48 (1H, t, *J* = 9.0 Hz) and 5.43 (1H, t, *J* = 5.1 Hz)], one oxygenated methyl [δ_H 3.68 (3H, s)], and two methyls [δ_H 1.92 (3H, s) and 1.05 (3H, d, *J* = 6.4 Hz)]. The ^{13}C NMR and DEPT spectra (**Table 2**) exhibited the presence of 23 carbons, including one carbonyl carbon (δ_C 196.7), eight quaternary carbons, six methines, five methylenes, and three methyls, indicating that **2** was also a clerodane diterpenoid. The analysis of 1D NMR data showed that **2** had the analogous planar structure as that crassifolin M (Wang et al., 2016), except for the absence of a carbonyl group (δ_C 195.7, C-6), but the presence of an oxygenated methine (δ_C 71.7) and an acetoxyl group (δ_C 170.1 and 21.1) in **2** and the chemical shifts of C-5, C-6, and C-7 shifted from δ_C 133.2, 195.7, 40.9 to δ_C 129.8, 71.7, 32.7, correspondingly. In addition, the acetoxyl group was attached to C-6, which was confirmed by ^1H–^1H COSY correlation between H-6 (δ_H 5.46) and H-7 (δ_H 2.10), together with HMBC cross peaks from H-22 (δ_H 1.92) to C-6 (δ_C 71.7)/C-21 (δ_C 170.1) (**Figure 1**). Moreover, the absolute configuration of **2** was determined as 4*S*, 6*S*, 8*R*, 9*R*, and 12*S* by a single X-ray diffraction experiment (**Figure 2**). Therefore, the structure of two was confirmed as showed in **Figure 3** and named as crassifolin R.

Compound **3**, a yellow oil, which had the molecular formula $C_{25}H_{34}O_6$ assigned by HR-ESI-MS (*m/z* 453.2234 $[M + Na]^+$, calcd for $C_{25}H_{34}O_6Na$, 453.2248). The IR spectrum indicated the presence of hydroxyl (3,419 $cm^{-}1$) and ester carbonyl groups (1718, 1,259 cm^{-1}). According to its ^1H NMR spectrum (**Table 1**), compound **3** exhibited the presence of characteristic signals for

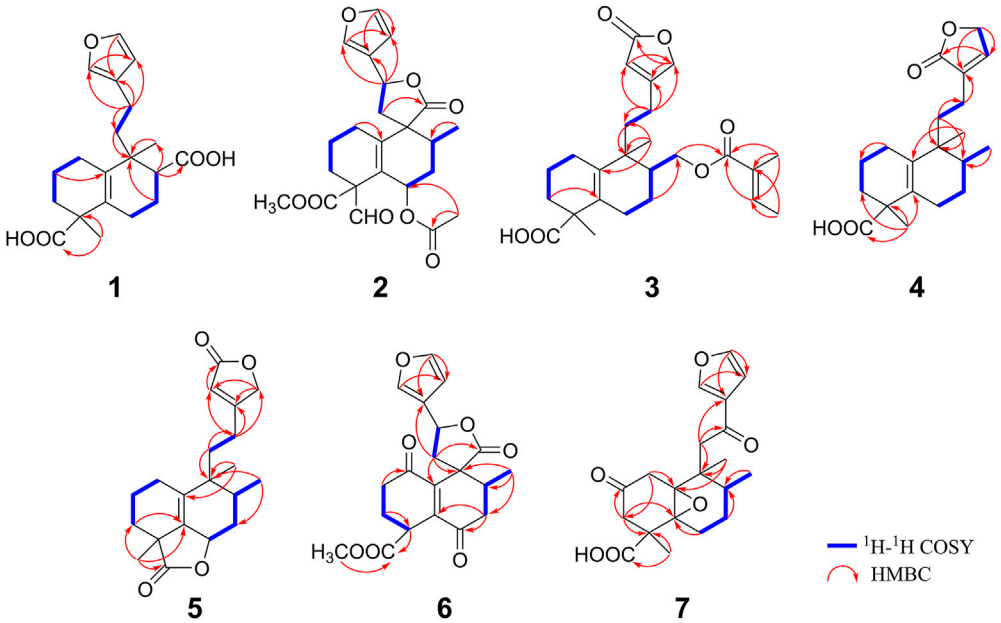

FIGURE 3 | Structures of compounds **1**–**12**.

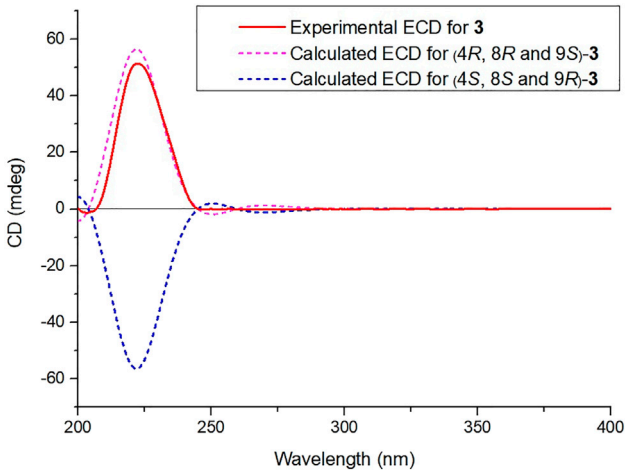

FIGURE 4 | Calculated and experimental ECD spectra of compound **3**.

two olefinic protons [δ_H 6.83 (1H, s, J = 7.0 Hz) and 5.82 (1H, s)], one methine [δ_H 1.78 (1H, m)], two oxygenated methylenes [δ_H 4.75 (2H, s), 4.38 (1H, dd, J = 11.0, 4.3 Hz), and 3.83 (1H, t, J = 9.2 Hz)], and four methyls [δ_H 1.78 (3H, s), 1.77 (3H, d, J = 7.0 Hz), 1.27 (3H, s), and 1.00 (3H, s)]. Comparison of 1D NMR data with those of crassifolin B (Wang et al., 2012) showed that they were similar to a typical clerodane diterpenoid skeleton. The differences between **3** and crassifolin B were the absence of a methyl (δ_C 16.2, C-17), but the presence of an oxygenated methylenes (δ_C 65.7) and a *cis*-2-methylbut-2-enoyloxy moiety (δ_C 168.4, 137.6, 128.8, 14.5, and 12.2). As a result, the chemical shifts of C-8 and C-17 shifted from δ_C 33.8 and 16.2 in crassifolin B to δ_C 39.0 and 65.7 in **3**, respectively. The presence of *cis*-2-methylbut-2-enoyloxy moiety was confirmed by the ^{1}H–^{1}H COSY correlation between H_3-24 (δ_H 1.77) and H-23 (δ_H 6.83), together with the HMBC cross peaks from H_3-24 to C-22 (δ_C 128.8)/C-23 (δ_C 137.6), from H_3-25 (δ_H 1.78) to C-21 (δ_C 168.4)/C-22 (**Figure 1**). In addition, the HMBC cross peaks from H-17 (δ_H 3.83) to C-21 indicated that the *cis*-2-methylbut-2-enoyloxy moiety was connected to C-17 (δ_C 65.7). Due to the influence of substituents on the chemical shift of olefinic hydrogen, the chemical shift of olefinic proton in *cis*-2-methylbut-2-enoyloxy moiety was greater than that of *trans*-2-methylbut-2-enoyloxy moiety (Pedro et al., 1989; Russel et al., 2014), and our ^{1}H NMR spectrum of **3** was consistent with *cis*-2-methylbut-2-enoyloxy moiety. Herein, the 2-methylbut-2-enoyloxy moiety in compound **3** was *cis*-configuration. Moreover, the absolute configuration of **3** was established by quantum-chemical ECD calculations. The experimental ECD spectrum of **3** showed a positive cotton effect at 224 nm ($\Delta\varepsilon$ +50.9), which was compared with the predicted ECD spectrum of (4*R*, 8*R*, 9*S*)-**3** and its enantiomer (**Figure 4**), indicating the absolute configuration of **3** was 4*R*, 8*R*, and 9*S*. Hence, the structure of **3** was established as **Figure 3** and named as crassifolin S.

Compound **4** was a white powder and showed an $[M + Na]^+$ ion peak at *m/z* 355.1869 (calcd for $C_{20}H_{28}O_4Na$, 355.1880) in the HR-ESI-MS spectrum, consistent with the molecular formula of $C_{20}H_{28}O_4$. The ^{1}H NMR spectrum of **4** (**Table 1**) exhibited one olefinic proton [δ_H 7.10 (1H, s)], one methine [δ_H 1.72 (1H, m)], and three methyls [δ_H 1.29 (3H, d, J = 6.8 Hz), 0.88 (3H, s), and 0.87 (3H, s)]. The NMR spectroscopic data of **4** resembled those of crassifolin B (Wang et al., 2012). A detailed comparison of the NMR spectra of **4** with crassifolin B indicated the connection

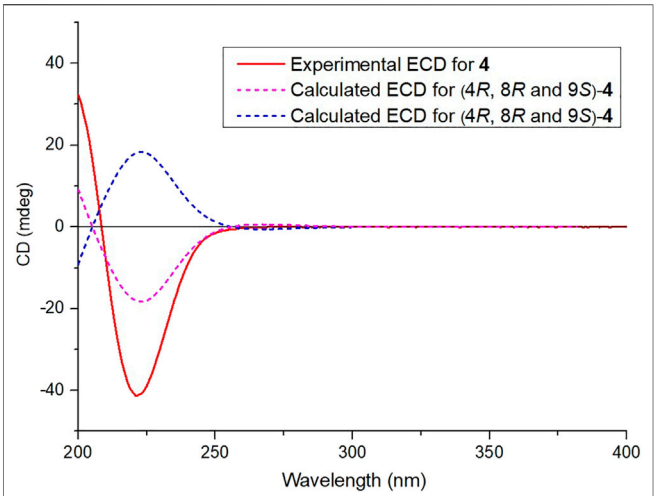

FIGURE 5 | Calculated and experimental ECD spectra of compound **4**.

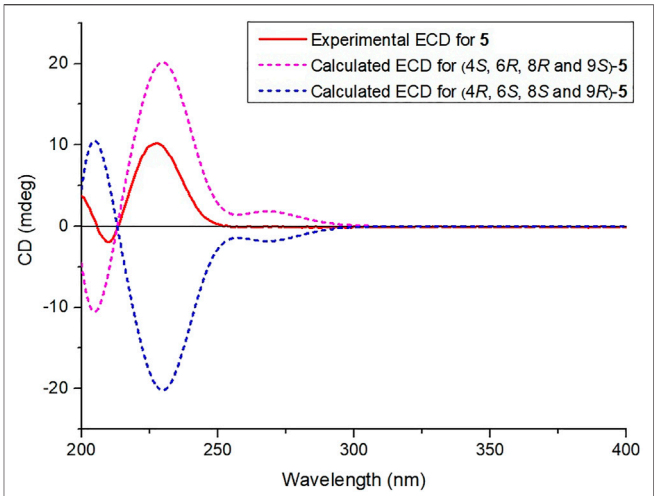

FIGURE 7 | Calculated and experimental ECD spectra of compound **5**.

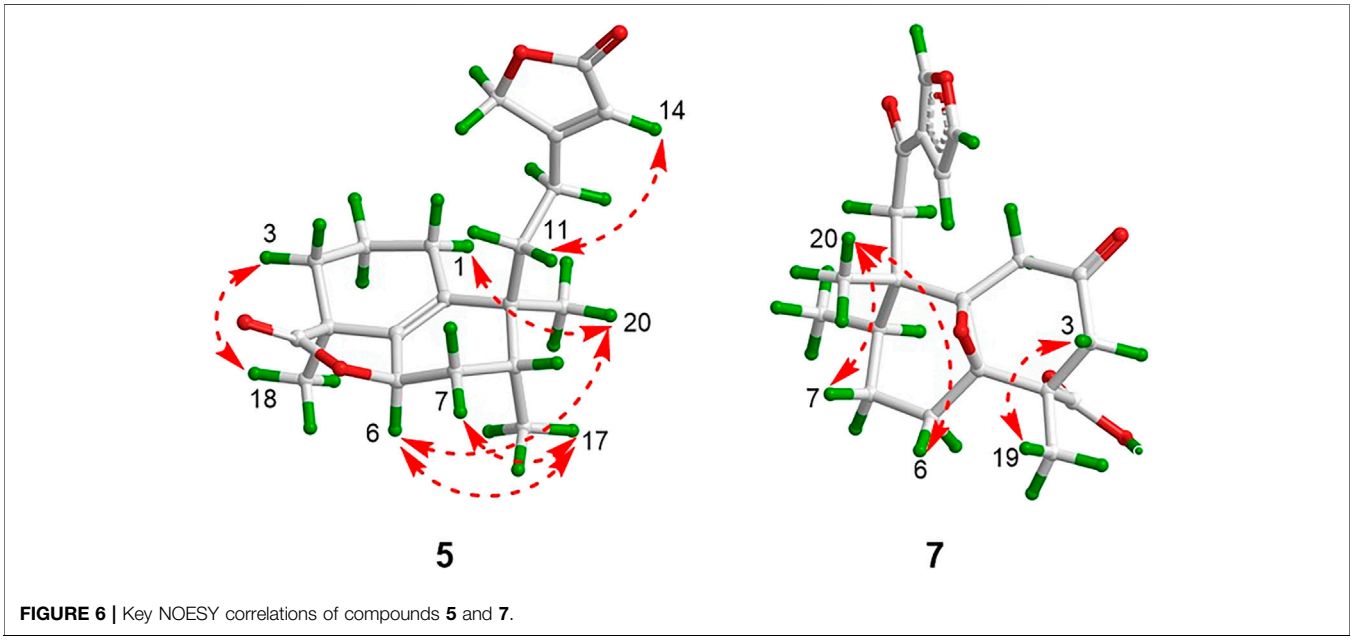

FIGURE 6 | Key NOESY correlations of compounds **5** and **7**.

position of C-12 and γ-lactone ring has changed, and the chemical shifts of C-12 to C-16 shifted from δ_C 23.7, 171.4, 115.1, 174.3, 73.3 to 20.5, 135.2, 174.5, 70.2, 143.9, respectively. The γ-lactone ring was confirmed by the ^{1}H–^{1}H COSY correlation between H-15 (δ_H 4.75) and H-16 (δ_H 7.10) along with the HMBC correlations from H-15 to C-13 (δ_C 135.2)/C-14 (δ_C 174.5)/C-16 (δ_C 143.9), from H-16 to C-14 (δ_C 174.5)/C-15 (δ_C 70.2). Moreover, the HMBC correlation from H-12 (δ_H 2.22) to C-13 was observed, which could confirm that the γ-lactone ring was attached to C-12 (**Figure 1**). The experimental ECD spectrum of **4** showed a positive cotton effect at 202 nm ($\Delta\varepsilon$ +35.0) and a negative cotton effect at 222 nm ($\Delta\varepsilon$ -42.1), which was similar to those of the calculated ECD spectrum for (4*R*, 8*R*, 9*S*)-**4** (**Figure 5**), suggested the absolute configuration of **4** is 4*R*, 8*R*, and 9*S*. Thus, compound **4** was named crassifolin T.

Compound **5** was isolated as a yellow oil and the molecular formula was determined to be $C_{20}H_{26}O_4$ by HR-ESI-MS (*m/z* 353.1710 [M + Na]$^+$, calcd for $C_{20}H_{24}O_6Na$, 353.1723). The IR spectrum showed characteristic ester carbonyl group (1743, 1,236 cm^{-}1). The ^{1}H NMR spectrum of **5** (**Table 1**) showed one olefinic proton [δ_H 5.82 (1H, s)], one oxygenated methine [δ_H 4.99 (1H, t, J = 8.1 Hz)], and three methyls [δ_H 1.32 (3H, s), 1.02 (3H, s), and 0.98 (3H, d, J = 7.2 Hz)]. The NMR spectra of **5** exhibited several similarities to crassifolin B (Wang et al., 2012). The main differences were the absence of a carboxylic acid group (δ_C 183.7, C-18) and a methylene (δ_C 27.8, C-6), but the presence

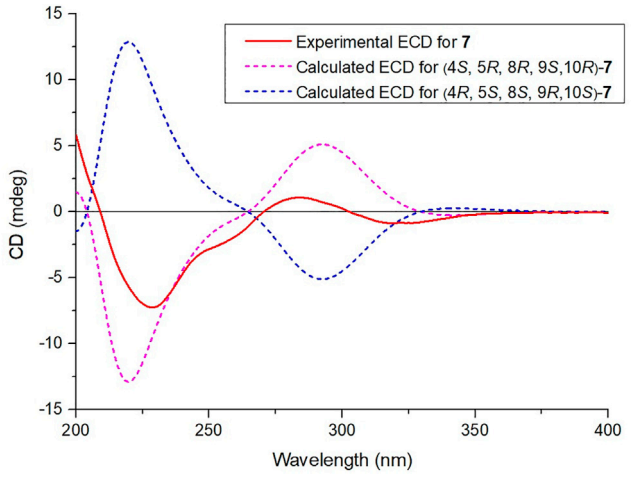

FIGURE 8 | Calculated and experimental ECD spectra of compound **7**.

of an ester group (δ_C 180.7) and a tertiary carbon bearing oxygen (δ_C 74.7), and the chemical shifts of C-4, C-6, and C-18 shifted from 47.8, 27.8, 183.7 to 41.7, 74.7, 180.7, respectively. This indicated that a lactone ring was formed between C-4 and C-6, which was confirmed by the ^{1}H–^{1}H COSY between H-6 (δ_H 4.99) and H-7 (δ_H 1.63) and the HMBC cross peak from H-19 (δ_H 1.32) to C-18. In addition, the key NOESY correlations between H-6 and H_3-17 (δ_H 0.98)/H_3-20 (δ_H 1.02), indicated that H-6 and H-17/H-20 were α-orientated (**Figure 6**). The experimental ECD spectrum of **5** exhibited a positive cotton effect at 226 nm ($\Delta\varepsilon$ +10.1) and a negative cotton effect at 206 nm ($\Delta\varepsilon$ -2.0), which was similar to those of the calculated ECD spectrum for (4*S*, 6*R*, 8*R*, 9*S*)-**5** (**Figure 7**). Thus, the structure of **5** was elucidated as 4*S*, 6*R*, 8*R*, 9*S* and compound **5** was named crassifolin U.

Compound **6**, a white powder, which had an $[M + H]^+$ ion peak at *m/z* 373.1283, consistent with the molecular formula $C_{20}H_{20}O_7$. The ^{1}H NMR spectrum of **6** (**Table 1**) showed three olefinic protons [δ_H 7.46 (1H, s), 7.44 (1H, s), and 6.40 (1H, s)], one oxygenated methine [δ_H 5.90 (t, J = 7.5 Hz)], and two methyls [δ_H 3.68 (s) and 1.14 (d, J = 7.0 Hz)]. The 1D NMR data of **6** were similar to those of spiro [furan-3(2*H*),1' (2'*H*)-naphtha-lene]-5'-carboxylic acid (Rodríguez and Jimeno, 2004), and the main differences were the absence of two methines [δ_C 50.2 (C-5) and 50.0 (C-10)] and a methylene (δ_C 28.1, C-1), but the presence of two olefinic carbons (δ_C 144.9 and 145.9) and a carbonyl group (δ_C 199.9). Thus, it indicated that two methines were replaced by two olefinic carbons and the methylene was replaced by a carbonyl group. These were confirmed by HMBC cross peaks from H-2 (δ_H 2.56) to C-1 (δ_C 199.9), from H-7 (δ_H 2.44) to C-5 (δ_C 144.9), and from H-11 (δ_H 2.71) to C-10 (δ_C 145.9) (**Figure 1**). The single crystal were obtained in a methanol system and subjected to an X-ray diffraction experiment with Cu Kα radiation and the crystal data [Flack parameter -0.06 (3), hooft parameter -0.03 (3)] determined the absolute configuration of **6** is 4, *8*, 9*R*, 12*S* (**Figure 1**). Compound **6** was named crassifolin V.

Compound **7** was obtained as yellow oil and had the molecular formula $C_{20}H_{24}O_6$. The ^{1}H NMR spectrum of **7** (**Table 1**) exhibited three olefinic protons [δ_H 8.05 (1H, s), 7.41 (1H, s), and 6.75 (1H, s)], one methine [δ_H 1.97 (m)], and three methyls [δ_H 1.20 (s), 1.08 (s) and 0.99 (d, J = 6.5 Hz)]. According to the 1D NMR spectroscopic data, the planar structure of compound **7** showed several similarities to methyl 5a,10a-epoxy-2,12-dioxo-13 (16),14-enthalimandien18-oate (Marcos et al., 2003), and the main differences were the absence of a carbethoxy group, but the presence of a carboxylic acid group (δ_C 176.6, C-18). Thus, it indicated the carbethoxy group was replaced by a carboxylic acid group in **7**, which was supported by the HMBC cross peaks from H-3 (δ_H 2.70) to C-4 (δ_C 51.0) and from H_3-19 (δ_H 1.08) to C-4/C-5/C-18 (**Figure 1**). Moreover, the NOESY correlation between H-8 and H_3-20 was not observed, which suggested that H_3-20 and H_3-17 were α-orientated; besides, the correlations of H_3-20/H-1α, of H-1α/H-3α, and of H-3α/H_3-19 indicated that H_3-20 and H_3-19 were α-orientated (**Figure 6**). The experimental ECD spectrum of **7** showed a positive cotton effect at 281 nm ($\Delta\varepsilon$ +2.1) and a negative cotton effect at 226 nm ($\Delta\varepsilon$ -7.0), which was similar to those of the calculated ECD spectrum for (4*S*, 5*R*, 8*R*, 9*S*, 10*R*)-**7** (**Figure 8**), suggested the absolute configuration of **7** is 4*S*, 5*R*, 8*R*, 9*S*, 10*R*. Compound **7** was named crassifolin W.

The Hypothetical Biosynthesis Pathway of New Compounds

In this paper, the new compounds we isolated from *C. crassifolius* all have the clerodane skeleton, which inspired us deriving their possible biosynthetic pathways.

Biogenetically, geranylgeranyl diphosphate is the precursor of diterpenoids, and it converts to the halimane system first (**Figure 9**). The carbocations participate in methyl migration, thereby generates some unsaturated halimanes represented by $\Delta^{5,10}$-halimane (Maslovskaya et al., 2019). In this process, $\Delta^{5,10}$-halimane underwent oxidation to produce crassifolin B, or underwent oxidation and esterification to gain crotohalimaneic acid. On the one side, crassifolin B underwent substitution, transfer, and esterification to afford crassifolin S (**3**), crassifolin T (**4**), and crassifolin U (**5**), respectively. On the other side, crotohalimaneic acid underwent oxidation to obtain crassifolin Q (**1**) and crotohalimoneic acid. Crotohalimoneic acid underwent esterification and oxidation to get crassifolin R (**2**) and crassifolin V (**6**). However, the stereochemistry of C-18 and C-19 of compound **7** and **8** were different for other isolated compounds, which implied their skeleton were different from others.

Anti-Inflammatory Activities of Compounds 1–5

According to previous reports (Wang et al., 2015; Maslovskaya et al., 2019), clerodane diterpenoids of *Croton crassifolius* had showed significant anti-inflammatory effect. Therefore, compounds (**1**–**5**) were tested for their activities against inflammatory cytokines IL-6 and TNF-α on RAW 264.7 cells. The cytotoxicities of compounds **1**–**5** were assessed by MTT assay on RAW 264.7 cells. As a result, compounds **1**–**5** at the concentration of 50 μM had no obvious cytotoxic activities on

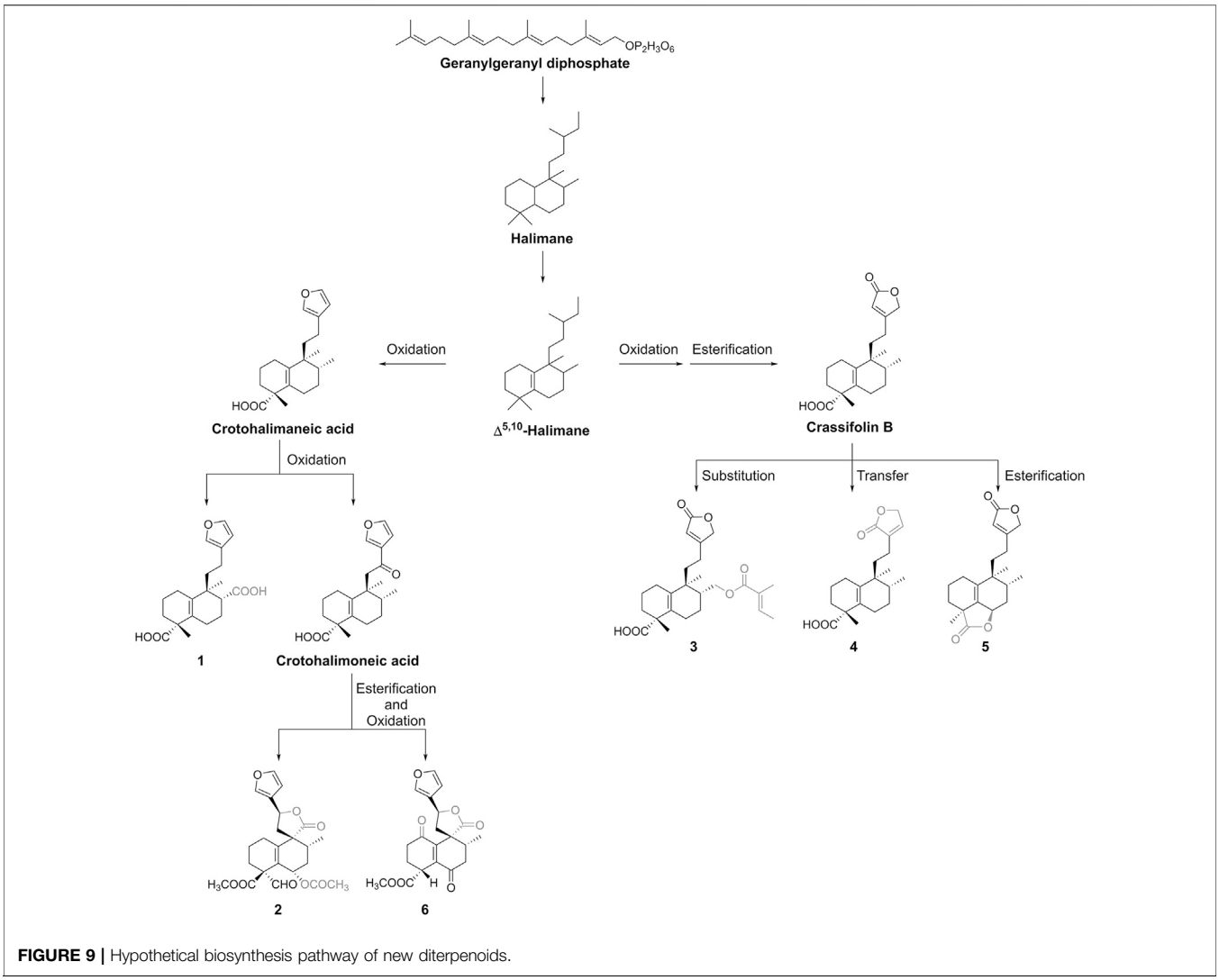

FIGURE 9 | Hypothetical biosynthesis pathway of new diterpenoids.

TABLE 3 | Anti-inflammatory activities of compounds **1**–**5** in LPS-stimulated RAW 264.7 cells.

Group	IL-6 (%)	TNF-α (%)
Blank	1.99 ± 2.89	1.68 ± 3.15
LPS	100 ± 2.23	100 ± 4.38
Dexamethasone	16.76 ± 2.98[a]	48.26 ± 3.68[a]
1	72.23 ± 3.84[b]	89.38 ± 3.54[b]
2	77.88 ± 5.21[b]	77.73 ± 4.22[b]
3	73.36 ± 1.06[b]	79.23 ± 3.21[b]
4	35.48 ± 2.15[a]	54.14 ± 1.55[a]
5	32.78 ± 1.99[a]	12.53 ± 1.92[a]

[a]$p < 0.001$.
[b]$p < 0.01$ vs *LPS group*.

RAW 264.7 cells after 24 h treatment. In this study, ELISA was applied to evaluate the levels of two inflammatory cytokines IL-6 and TNF-α. As shown in **Table 3**, compounds **1**–**5** showed the secretion levels of IL-6 ranging from 32.78 to 77.88%, and the TNF-α ranging from 12.53 to 89.38%. Among them, compound **5** showed the most significant secretion levels of IL-6 and TNF-α at 32.78 and 12.53%, respectively.

Anti-Angiogenesis Activities of Compounds 1–5

Considering the potential anti-angiogenesis activity of diterpenoids from *C. crassifolius* (Huang et al., 2016; Wang et al., 2016), compounds **1**–**5** were evaluated for their anti-angiogenesis activities by using tube formation assay in HUVECs. In this assay, we evaluated anti-angiogenesis activities of compounds according to junction densities, vessel percentage areas, and average vessel lengths. Experimental results (**Figure 10** and **Supplementary Figure S71**–**Figure S74**) showed that compounds **1**–**5** significantly inhibited angiogenesis by reducing the number of cavities formation. Among these compounds, compound **5** showed the strongest anti-angiogenesis effect, resulting in half maximal inhibitory concentration (IC_{50}) values of junction densities, vessel percentage areas, and average vessel lengths of 7.20 ± 2.23,

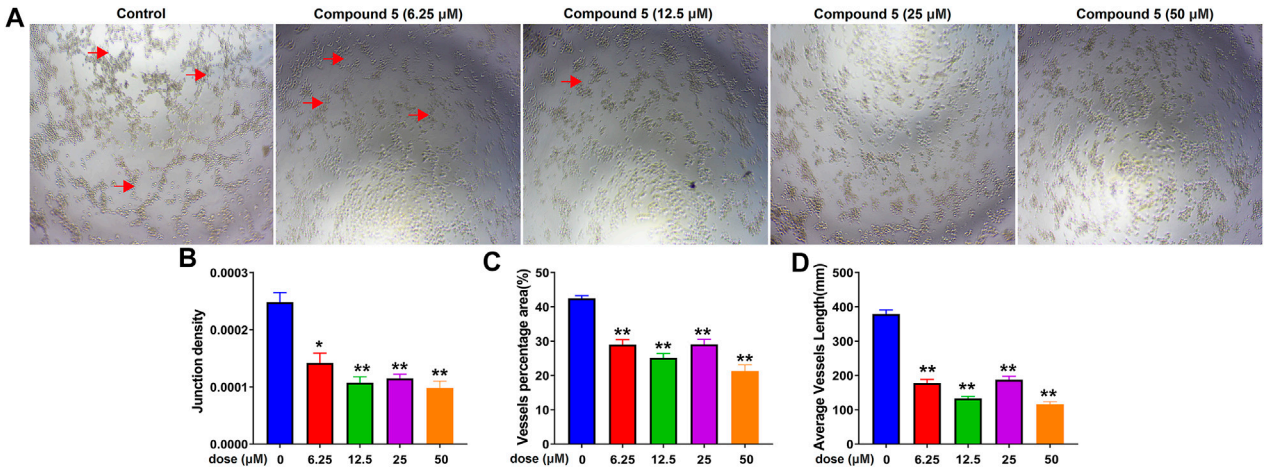

FIGURE 10 | The inhibitory effect of compound **5** on angiogenesis. **(A)** Bright field images of HUVECs seeded on Matrigel for 24 h after treatment at different doses of compound **5**; red arrows indicated the cavities formation during angiogenesis. **(B)**, **(C)**, **(D)** Quantitative analysis on junction densities, vessel percentage areas, and average vessel lengths, respectively. Data are expressed as mean ± SD of three independent experiments. $^{*}p < 0.05$, $^{**}p < 0.005$, $^{***}p < 0.001$ compared with the control group.

48.27 ± 1.98, and 8.62 ± 2.89 μM, respectively. These results revealed that compounds **1**–**5** significantly inhibited the tube formation of HUVECs and showed their anti-angiogenesis activities.

According to the results of experiments with biological activities, crassifolin U (**5**) showed better inhibitory activities in both inflammation and angiogenesis. Compared with other compounds, there were more lactone rings in the structure of compound **5**, which implied that the lactone ring may be an important functional group for anti-inflammatory and anti-angiogenesis activities.

CONCLUSION

In conclusion, seven new clerodane diterpenoids were isolated from the roots of *C. crassifolius*. Their structures were identified by comprehensive analysis of spectroscopic data and X-ray crystallography. The anti-inflammatory activities of compounds **1**–**5** was determined according to two inflammatory cytokines IL-6 and TNF-α, and compound **5** showed the strongest anti-inflammatory ability with the secretion of IL-6 and TNF-α at 32.78 and 12.78%, respectively. Moreover, the results of experiments on anti-angiogenesis activities showed compounds **1**–**5** inhibited angiogenesis obviously and compound **5** showed the strongest anti-angiogenesis effect with doses in the range of 6.25–50 μM.

EXPERIMENTAL

General Experimental Procedures

UV spectra were measured by a JASCO V-550 UV/VIS spectrophotometer (JASCO, Tokyo, Japan). IR spectra were measured by a JASCO FT/IR-480 plus FT-IR spectrometer with KBr pellets (JASCO, Tokyo, Japan). A JASCO P-1020 polarimeter was used for measuring the optical rotations (JASCO, Tokyo, Japan). HRESIMS data were accomplished using an Agilent 6210 ESI/TOF mass spectrometer (Agilent, Massachusetts, United States). ECD spectra were measured by an Applied Photophysics Chirascan plus CD (Applied Photophysics, United Kingdom). NMR spectra were obtained on a Bruker AV-400 spectrometer with TMS as the internal standard (Bruker, Karlsruhe, Germany), and the chemical shifts (δ) are expressed in ppm and coupling constants (J) in Hz. For column chromatography (CC), silica gel (200–300 mesh, Qingdao Marine Chemical Plant, Qingdao, P. R. China), ODS (50 μm, YMC, Kyoto, Japan), and Sephadex LH-20 (Pharmacia Biotech, Uppsala, Sweden) were used. Silica gel GF_{254} plates (Yantai Chemical Industry Research Institute, Yantai, China) were used for thin-layer chromatography (TLC). HPLC separations were performed using a COSMOSIL C_{18} preparative column (5 μm, 20 × 250 mm). All chemical reagents were purchased from Shandong Yuwang Chemical Company (Shandong, P. R. China).

Plant Material

The roots of *C. crassifolius* were collected from Yulin City, Guangxi province of China. The species was identified by Professor Guangxiong Zhou of Jinan University. A voucher specimen (No. 20200713) is deposited in the Institute of Traditional Chinese Medicine and Natural Products of Jinan University.

Extraction and Isolation

The air-dried roots of *C. crassifolius* (20.0 kg) were extracted three times with 95% ethanol at room temperature. The solution was evaporated under reduced pressure to get a residue (1,500.0 g), which was suspended in water and then partitioned with petroleum ether (PE, 55.6 g), dichloromethane (CH_2Cl_2,

1,005.3 g), and ethyl acetate (EtOAc, 180.9 g). The dichloromethane extract was chromatographed on a silica gel column chromatograph using the petroleum ether/ethyl acetate (100:0→0:100, v/v) solvent system. The fractions were examined by TLC and combined to give eight fractions (Fr. 1–Fr. 8). Fr. 6 (72.4 g) was subjected to a reversed silica gel column chromatography eluting with MeOH/H_2O (30:70→100:0, v/v) to afford six subfractions (Fr. 6A–Fr. 6F). Fr. 6C (6.1 g) was separated by Sephadex LH-20 ($CHCl_3$/MeOH, 1:1, v/v) and further purified by the preparative HPLC (MeOH/H_2O, 70:30, v/v) to yield compounds **1** (20.2 mg), **2** (26.8 mg), **3** (23.6 mg), and **8** (19.8 mg). F. 6D (10.2 g) was purified by Sephadex LH-20 ($CHCl_3$/MeOH, 1:1, v/v) to obtain compounds **4** (232.6 mg), **5** (22.4 mg), **6** (230.8 mg), **9** (332.5 mg), and **10** (33.8 mg). Fr. 6E (5.5 g) was separated by the preparative HPLC (MeOH/H_2O, 60: 40, v/v) to afford compound **7** (30.7 mg), **10** (35.5 mg), **11** (19.7 mg), and **12** (22.9 mg).

Characterization of Compounds 1–7

Crassifolin Q (**1**): colorless crystal (MeOH); mp 139–140°C; $[\alpha]_D^{25}$ +36.8 (*c* 1.0, MeOH); HR-ESI-MS *m/z* 369.1660 $[M + Na]^+$ (calcd for $C_{19}H_{24}O_7Na$, 369.1672); UV (MeOH) λ_{max} 200 nm; IR (KBr) ν_{max} 3,463, 2,956, 1710, 1,461, 1,355, 1,203, 1,037 cm^{-1}; ^1H and ^{13}C NMR data see **Tables 1**, **2**.

Crassifolin R (**2**): colorless crystal (MeOH); mp 146–147°C; $[\alpha]_D^{25}$ +57.9 (*c* 1.0, MeOH); HR-ESI-MS *m/z* 453.1506 $[M + Na]^+$ (calcd for $C_{19}H_{24}O_7Na$, 453.1520); UV (MeOH) λ_{max} 201 nm; IR (KBr) ν_{max} 3,133, 2,965, 1737, 1,450, 1,249, 1,164, 1,018, 808, 748, 603 cm^{-1}; ^1H and ^{13}C NMR data see **Tables 1**, **2**.

Crassifolin S (**3**): yellow oil; $[\alpha]_D^{25}$ +33.9 (*c* 1.0, MeOH); HR-ESI-MS *m/z* 453.2234 $[M + Na]^+$ (calcd for $C_{19}H_{24}O_7Na$, 453.2248); UV (MeOH) λ_{max} 203 nm; IR (KBr) ν_{max} 3,419, 2,942, 1718, 1,446, 1,357, 1,259, 1,155, 1,027, 867 cm^{-1}; ECD (MeOH) λ_{max} ($\Delta\varepsilon$) 224 (+50.9) nm; ^1H and ^{13}C NMR data see **Tables 1**, **2**.

Crassifolin T (**4**): white powder; mp 135–136°C; $[\alpha]_D^{25}$ -48.6 (*c* 1.0, MeOH); HR-ESI-MS *m/z* 355.1869 $[M + Na]^+$ (calcd for $C_{19}H_{24}O_7Na$, 355.1880); UV (MeOH) λ_{max} 201 nm; IR (KBr) ν_{max} 2,946, 2,657, 1735, 1,448, 1,280, 1,195, 1,056, 923, 842 cm^{-1}; ECD (MeOH) λ_{max} ($\Delta\varepsilon$) 201 (+35.0), 224 (−42.1) nm; ^1H and ^{13}C NMR data see **Tables 1**, **2**.

Crassifolin U (**5**): yellow oil; $(\alpha)_D^{25}$ +42.5 (*c* 1.0, MeOH); HR-ESI-MS *m/z* 353.1710 $(M + Na)^+$ (calcd for $C_{19}H_{24}O_7Na$, 353.1723); UV (MeOH) λ_{max} 202 nm; IR (KBr) ν_{max} 2,935, 1743, 1,639, 1,448, 1,236, 1,164, 1,014, 869 cm^{-1}; ECD (MeOH) λ_{max} ($\Delta\varepsilon$) 226 (+10.1), 206 (−2.0) nm; ^1H and ^{13}C NMR data see **Tables 1**, **2**.

Crassifolin V (**6**): white powder; mp 144–147°C; $[\alpha]_D^{25}$ +22.7 (*c* 1.0, MeOH); HR-ESI-MS *m/z* 373.1283 $[M + H]^+$ (calcd for $C_{20}H_{21}O_7$, 373.1282); UV (MeOH) λ_{max} 203 nm; IR (KBr) ν_{max} 2,948, 2,898, 1745, 1,679, 1,434, 1,201, 1,160, 1,025 cm^{-1}; ECD (MeOH) λ_{max} ($\Delta\varepsilon$) 263 (+42.5), 225 (−28.1) nm; ^1H and ^{13}C NMR data see **Tables 1**, **2**.

Crassifolin W (**7**): yellow oil; $(\alpha)_D^{25}$ -32.5 (*c* 1.0, MeOH); HR-ESI-MS *m/z* 361.1644 $[M + H]^+$ (calcd for $C_{20}H_{25}O_6$, 361.1646); UV (MeOH) λ_{max} 200 nm; IR (KBr) ν_{max} 3,436, 2,942, 2,879, 1783, 1720, 1,666, 1,562, 1,511, 1,390, 1,253, 1,155, 871 cm^{-1}; ECD (MeOH) λ_{max} ($\Delta\varepsilon$) 280 (+2.1), 226 (−7.0) nm; ^1H and ^{13}C NMR data see **Tables 1**, **2**.

X-Ray Crystallographic Data of 1, 2, and 6

Crystal data for **1**: $C_{20}H_{26}O_5$, M = 346.41, orthorhombic, space group $P2_12_12_1$, a = 9.129 (5) Å, b = 24.185 (5) Å, c = 17.080 (5) Å, V = 3,771.66 (2) $Å^3$, Z = 8, d_x = 1.220 g/cm^3, F (000) = 1,488.0, μ(Cu Kα) = 0.708 mm^{-1}. Data collection was performed on a Gemini S Ultra using graphite monochromatic radiation (λ = 1.54184 Å), 2,188 unique reflections were collected to θ_{max} = 74.98°, where 3,898 reflections were observed [$F^2 > 2\sigma(F^2)$]. The structure was solved by direct methods (SHELXS 97) and refined by full matrix least-squares on F^2. Final R = 0.0525, R_w = 0.1726, and S = 1.046. Crystallographic data for this structure have been deposited with the Cambridge Crystallographic Data Center as CCDC 2078339 for crassifolin Q (**1**).

Crystal data for **2**: $C_{23}H_{26}O_8$, M = 430.44, orthorhombic, space group $P2_12_12_1$, a = 8.2304 (1) Å, b = 10.0512 (2) Å, c = 25.6929 (4) Å, V = 2,125.46 (6) $Å^3$, Z = 4, d_x = 1.345 g/cm^3, F (000) = 912.0, μ(Cu Kα) = 0.850 mm^{-1}. Data collection was performed on a Gemini S Ultra using graphite monochromatic radiation (λ = 1.54184 Å), 2,479 unique reflections were collected to θ_{max} = 73.93°, where 4,308 reflections were observed [$F^2 > 2\sigma(F^2)$]. The structure was solved by direct methods (SHELXS 97) and refined by full matrix least-squares on F^2. Final R = 0.0357, R_w = 0.1174, and S = 1.026. Crystallographic data for this structure have been deposited with the Cambridge Crystallographic Data Center as CCDC 2078342 for crassifolin R (**2**).

Crystal data for **6**: $C_{20}H_{21}O_7$, M = 372.12, orthorhombic, space group $P2_12_12_1$, a = 6.3217 (4) Å, b = 7.3898 (8) Å, c = 10.1209 (7) Å, V = 440.11 (7) $Å^3$, Z = 1, d_x = 1.405 g/cm^3, F (000) = 196.0, μ(Cu Kα) = 0.895 mm^{-}1. Data collection was performed on a Gemini S Ultra using graphite monochromatic radiation (λ = 1.54184 Å), 2,998 unique reflections were collected to θ_{max} = 74.455°, where 3,600 reflections were observed [$F^2 > 2\sigma(F^2)$]. The structure was solved by direct methods (SHELXS 97) and refined by full matrix least-squares on F^2. Final R = 0.0488, R_w = 0.1459, and S = 1.108. Crystallographic data for this structure have been deposited with the Cambridge Crystallographic Data Center as CCDC 2093010 for crassifolin V (**6**).

Cell Viability Assay

RAW 264.7 cells were purchased from American Type Culture Collection. Cells were seeded in a 96-well plate at the density of 5 × 10^4 cells/ml for 24 h and then the cells were treated with compounds **1**–**5** for 24 h. The mixture was then removed and each well of the plates was incubated with 30 μl of MTT (5 mg/ml) at 37°C for 4 h. After complete removal of the supernatant, DMSO (100 μl/well) was added into the plates to dissolve the formazan produced in the cells. The absorbance was recorded by a microplate reader at 570 nm.

Assay of Enzyme-Linked Immunosorbent Assay

To quantify the level of proinflammatory cytokines, RAW 264.7 cells were placed in a 24-well plate at a density of 2 × 10^5/ml for 24 h. Then, the cells were pretreated with 50 μM of isolated compounds **1**–**5** for 12 h before stimulation with LPS for another 12 h. The level of IL-6 and TNF-α in cell supernatants were quantified with ELISA kits according to the manufacturer's protocols. In this assay, data were expressed as mean ± SD. Statistical significance was considered when p value <0.05.

Tube Formation Assay

The effects of compounds on angiogenesis of endothelial cell *in vitro* were tested using the tube formation assay on Matrigel (BD Biosciences, MA, United States). In this assay, Matrigel (50 μl) was added to the wells of a pre-chilled 96-well plate and put at 37°C for 30 min to congeal. The prepared HUVECs with a density of 2×10^5 cells/well was added and treated with isolated compounds **1**–**5** at different concentrations. The image of tube formation was collected after 8 h. The junction densities, vessel percentage areas, and average vessel lengths were measured and recorded. In this assay, data were expressed as mean ± SD of three independent experiments. $^{*}p < 0.05$, $^{**}p < 0.01$, $^{***}p < 0.001$ compared with the control group.

DATA AVAILABILITY STATEMENT

The original contributions presented in the study are included in the article/Supplementary files, further inquiries can be directed to the corresponding authors.

AUTHOR CONTRIBUTIONS

CL, XS, and WY performed the experiments. CL, ZZ, and QT identified the structures. QT, WW, XZ, and ZW performed the ECD calculation. YL, YZ, and GW conceived and designed the experiments. CL wrote the paper. HZ and CL deduced the biosynthesis pathway. YZ and ZZ revised the paper. All authors have approved the final version of the manuscript.

FUNDING

This work was supported by grants from the National Natural Science Foundation of China (Nos. 81803376, 81973190), the Guangdong Basic and Applied Basic Research Foundation (Nos. 2020B1515020033, 2020A1515110415), the Natural Science Foundation of Guangdong Province (No. 2018B030311020), the Local Innovative and Research Teams Project of Guangdong Pearl River Talents Program (2017BT01Y036), the Pearl River S&T Nova Program of Guangzhou (201906010069), and the high performance public computing service platform of Jinan University.

SUPPLEMENTARY MATERIAL

The Supplementary Material for this article can be found online at: https://www.frontiersin.org/articles/10.3389/fchem.2021.733350/full#supplementary-material

REFERENCES

Boonyarathanakornkit, L., Che, C.-t., Fong, H., and Farnsworth, N. (1988). Constituents of Croton Crassifolius Roots. *Planta Med.* 54, 61–63. doi:10.1055/s-2006-962339

Bryant, T. (1868). Remarks on Some Cases of Inflammation of the Breast Simulating Cancer. *BMJ* 2, 608–609. doi:10.1136/bmj.2.415.608

Campos, M. C. O., Salomão, K., Castro-Pinto, D. B., Leon, L. L., Barbosa, H. S., Maciel, M. A. M., et al. (2010). *Croton Cajucara* Crude Extract and Isolated Terpenes: Activity on *Trypanosoma Cruzi*. *Parasitol. Res.* 107, 1193–1204. doi:10.1007/s00436-010-1988-6

Corlay, N., Delang, L., Girard-Valenciennes, E., Neyts, J., Clerc, P., Smadja, J., et al. (2014). Tigliane Diterpenes from *Croton Mauritianus* as Inhibitors of Chikungunya Virus Replication. *Fitoterapia* 97, 87–91. doi:10.1016/j.fitote.2014.05.015

Dao, T.-T., Lee, K.-Y., Jeong, H.-M., Nguyen, P.-H., Tran, T. L., Thuong, P.-T., et al. (2011). Ent-Kaurane Diterpenoids fromCroton tonkinensisStimulate Osteoblast Differentiation. *J. Nat. Prod.* 74, 2526–2531. doi:10.1021/np200667f

Fernandes, V. C., Pereira, S. I. V., Coppede, J., Martins, J. S., Rizo, W. F., Beleboni, R. O., et al. (2013). The Epimer of Kaurenoic Acid from *Croton Antisyphiliticus* Is Cytotoxic toward B-16 and HeLa Tumor Cells through Apoptosis Induction. *Genet. Mol. Res.* 12, 1005–1011. doi:10.4238/2013.April.2.16

Francescone, R., Hou, V., and Grivennikov, S. I. (2014). Microbiome, Inflammation, and Cancer. *Cancer J.* 20, 181–189. doi:10.1097/PPO.0000000000000048

Huang, H.-L., Qi, F.-M., Yuan, J.-C., Zhao, C.-G., Yang, J.-W., Fang, F.-H., et al. (2014a). Labdane-type Diterpenoids from *Croton Laevigatus*. *RSC Adv.* 4, 39530–39540. doi:10.1039/c4ra04863f

Huang, W. H., Li, G. Q., Li, J. G., Ge, W., Chung, H. Y., Wang, G. C., et al. (2014b). Two New Clerodane Diterpenoids from *Croton Crassifolius*. *Heterocycles* 89, 1585–1593. doi:10.3987/COM-13-12882

Khanitha, P., and Damrong, S. (2011). Clerodane Diterpenoids and a Trisubstituted Furan from *Croton Oblongifolius*. *Phytochem. Lett.* 4, 147–150. doi:10.1016/j.phytol.2011.02.004

Li, F., Zhang, D.-B., Li, J.-T., He, F.-J., Zhu, H.-L., Li, N., et al. (2019). Bioactive Terpenoids from *Croton Laui*. *Nat. Product. Res.* 9, 1–9. doi:10.1080/14786419.2019.1675062

Li, H.-H., Qi, F.-M., Dong, L.-L., Fan, G.-X., Che, J.-M., Guo, D.-D., et al. (2014). Cytotoxic and Antibacterial Pyran-2-One Derivatives from *Croton Crassifolius*. *Phytochem. Lett.* 10, 304–308. doi:10.1016/j.phytol.2014.10.022

Liu, C.-P., Xu, J.-B., Zhao, J.-X., Xu, C.-H., Dong, L., Ding, J., et al. (2014). Diterpenoids from *Croton Laui* and Their Cytotoxic and Antimicrobial Activities. *J. Nat. Prod.* 77, 1013–1020. doi:10.1021/np500042c

Marcos, I. S., Hernández, F. A., Sexmero, M. J., DÍez, D., Basabe, P., Pedrero, A. B., et al. (2003). Synthesis and Absolute Configuration of (−)-chettaphanin I and (−)-chettaphanin II. *Tetrahedron* 59, 685–694. doi:10.1016/s0040-0(02)01564-8

Mariana, M. B. A., Francisco, C. M. C., Catia, A. A., Humberto, R. B., Rafael, S. D., Galba, M. C., et al. (2013). Antioxidant and Antimicrobial Activities of 7-Hydroxycalamenene-Rich Essential Oils from *Croton Cajucara* Benth. *Molecules* 18, 1128–1137. doi:10.3390/molecules18011128

Martha, S. F., Claudia, P. C., Sandra, J. M., Fabio, A., and Coralia, O. (2011). Cytotoxic Labdane Diterpenoids Isolated from the Hexane Fraction of the *Croton Stipuliformis* Stem Bark. *Vitae* 18, 173–182.

Martinsen, A., Baccelli, C., Navarro, I., Abad, A., Quetin-Leclercq, J., and Morel, N. (2010). Vascular Activity of a Natural Diterpene Isolated from *Croton Zambesicus* and of a Structurally Similar Synthetic Trachylobane. *Vasc. Pharmacol.* 52, 63–69. doi:10.1016/j.vph.2009.11.002

Maslovskaya, L. A., Savchenko, A. I., Gordon, V. A., Reddell, P. W., Pierce, C. J., Boyle, G. M., et al. (2019). New Halimanes from the Australian Rainforest Plant *Croton Insularis*. *Eur. J. Org. Chem.* 2019, 1058–1060. doi:10.1002/ejoc.201801548

Maslovskaya, L. A., Savchenko, A. I., Gordon, V. A., Reddell, P. W., Pierce, C. J., Parsons, P. G., et al. (2015). EBC-316, 325-327, and 345: New Pimarane Diterpenes from *Croton insularis* Found in the Australian Rainforest. *Aust. J. Chem.* 68, 652–659. doi:10.1071/CH14550

Moses, C., Garcia-Bloj, B., Harvey, A. R., and Blancafort, P. (2018). Hallmarks of Cancer: The CRISPR Generation. *Eur. J. Cancer* 93, 10–18. doi:10.1016/j.ejca.2018.01.002

Nakatsu, T., Ito, S., and Kawashima, T. (1981). Mallotucin C and D, Two Diterpenic Lactones from *Mallotus Repandus*. *Heterocycles* 15, 241–244. doi:10.3987/S-1981-01-0241

Nina, C., Leen, D., Emmanuelle, G. V., Johan, N., Patricia, C., Jacqueline, S., et al. (2014). Tigliane Diterpenes from *Croton Mauritianus* as Inhibitors of Chikungunya Virus Replication. *Fitoterapia* 97, 87–91. doi:10.1016/j.fitote.2014.05.015

Qiu, M., Cao, D., Gao, Y., Li, S., Zhu, J., Yang, B., et al. (2016). New Clerodane Diterpenoids from *Croton Crassifolius*. *Fitoterapia* 108, 81–86. doi:10.1016/j.fitote.2015.11.016

Rodríguez, B., and Jimeno, M. L. (2004). 1H and13C NMR Spectral Assignments and Conformational Analysis of 14 19-Nor-Neoclerodane Diterpenoids. *Magn. Reson. Chem.* 42, 605–616. doi:10.1002/mrc.1384

Sun, Y., Wang, M., Ren, Q., Li, S., Xu, J., Ohizumi, Y., et al. (2014). Two Novel Clerodane Diterpenenes with NGF-Potentiating Activities from the Twigs of *Croton Yanhuii*. *Fitoterapia* 95, 229–233. doi:10.1016/j.fitote.2014.03.012

Suwancharoen, S., Chonvanich, O., Roengsumran, S., and Pornpakakul, S. (2012). *Seco*-kaurane Skeleton Diterpenoids from *Croton Oblongifolius*. *Chem. Nat. Compd.* 48, 583–586. doi:10.1007/s10600-012-0317-y

Takashi, K., Tokyo, T. N., and Yoshimasa, F. (1976). Diterpenic Lactones of *Mallotus Repandus*. *Heterocycles* 5, 227–232.

Wang, G.-C., Li, J.-G., Li, G.-Q., Xu, J.-J., Wu, X., Ye, W.-C., et al. (2012). Clerodane Diterpenoids from *Croton Crassifolius*. *J. Nat. Prod.* 75, 2188–2192. doi:10.1021/np300636k

Wang, J.-F., Yang, S.-H., Liu, Y.-Q., Li, D.-X., He, W.-J., Zhang, X.-X., et al. (2015). Five New Phorbol Esters with Cytotoxic and Selective Anti-inflammatory Activities from *Croton Tiglium*. *Bioorg. Med. Chem. Lett.* 25, 1986–1989. doi:10.1016/j.bmcl.2015.03.017

Wang, J.-J., Chung, H. Y., Zhang, Y.-B., Li, G.-Q., Li, Y.-L., Huang, W.-H., et al. (2016). Diterpenoids from the Roots of *Croton Crassifolius* and Their Anti-angiogenic Activity. *Phytochemistry* 122, 270–275. doi:10.1016/j.phytochem.2015.12.011

Young, H. S., Myung, S. L., Eun, Y. C., Phuong, T. T., Nguyen, M. K., and Song, I. S. (2013). An *Ent*-Kaurane Diterpenoid from *Croton Tonkinensis* Induces Apoptosis by Regulating AMP-Activated Protein Kinase in SK-HEP1 Human Hepatocellular Carcinoma Cells. *Biol. Pharm. Bull.* 36, 158–164. doi:10.1248/bpb.b12-00873

Yuan, Q.-Q., Tang, S., Song, W.-B., Wang, W.-Q., Huang, M., and Xuan, L.-J. (2017). Crassins A-H, Diterpenoids from the Roots of Croton Crassifolius. *J. Nat. Prod.* 80, 254–260. doi:10.1021/acs.jnatprod.6b00425

Zhang, D.-B., Tang, Z.-S., Xie, P., Liang, Y.-N., Yu, J.-G., Zhang, Z., et al. (2019). A Pair of New Neo-Clerodane Diterpenoid Epimers from the Roots of *Croton Crassifolius* and Their Anti-inflammatory. *Nat. Product. Res.* 34, 2945–2951. doi:10.1080/14786419.2019.1601193

Zhang, X.-L., Wang, L., Li, F., Yu, K., and Wang, M.-K. (2013). Cytotoxic Phorbol Esters of *Croton Tiglium*. *J. Nat. Prod.* 76, 858–864. doi:10.1021/np300832n

Conflict of Interest: The authors declare that the research was conducted in the absence of any commercial or financial relationships that could be construed as a potential conflict of interest.

Publisher's Note: All claims expressed in this article are solely those of the authors and do not necessarily represent those of their affiliated organizations, or those of the publisher, the editors and the reviewers. Any product that may be evaluated in this article, or claim that may be made by its manufacturer, is not guaranteed or endorsed by the publisher.